

A deep learning approach for robust, multi-oriented and curved text detection

Ramin Ranjbarzadeh¹, Saeid Jafarzadeh Ghoushchi², Shokofeh Anari³, Sadaf Safavi⁴, Nazanin Tataei Sarshar⁵, Erfan Babaee Tirkolaee^{6,*}, Malika Bendeche⁷

¹ School of Computing, Faculty of Engineering and Computing, Dublin City University, Ireland.

ramin.ranjbarzadehkondrood2@mail.dcu.ie

² Faculty of Industrial Engineering, Urmia University of Technology, Urmia, Iran.

s.jafarzadeh@uut.ac.ir

³ Department of Accounting, Economic and Financial Sciences, Islamic Azad University, South Tehran Branch, Tehran, Iran.

shokofehanarii@gmail.com

⁴ Department of Computer Engineering, Mashhad Branch, Islamic Azad University, Mashhad, Iran.

sf.safavi@gmail.com

⁵ Department of engineering, Islamic Azad university, Tehran north Branch, Tehran, Iran.

ab.tataee@gmail.com

⁶ Department of Industrial Engineering, Istinye University, Istanbul, Turkey.

erfan.babaee@istinye.edu.tr

⁷ Lero & ADAPT Research Centres, School of Computer Science, University of Galway, Ireland.

malika.bendeche@universityofgalway.ie

Abstract

Background Automatic text localization and segmentation in a normal environment with vertical or curved texts are core elements of numerous tasks comprising the identification of vehicles and self-driving cars, and preparing significant information from real scenes to visually impaired people. Nevertheless, texts in the real environment can be discovered with a high level of angles, profiles, dimensions, and colors which is an arduous process to detect.

Methods In this paper, a new framework based on a convolutional neural network (CNN) is introduced to obtain high efficiency in detecting text even in the presence of a complex background. Due to using a new inception layer and an improved ReLU layer, an excellent result is gained to detect text even in the presence of complex backgrounds. At first, four new m.ReLU layers are employed to explore low-level visual features. The new m.ReLU building block and Inception layer are optimized to detect vital information maximally.

Results The effect of stacking up inception layers (kernels with the dimension of 3×3 or bigger) is explored and it is demonstrated that this strategy is capable of obtaining mostly varying-sized texts further successfully than a linear chain of Convolution Layers (Conv layers). The suggested text detection algorithm is conducted in four well-known databases, namely ICDAR 2013, ICDAR

40 2015, ICDAR 2017, and ICDAR 2019.

41 **Conclusions** Text detection results on all mentioned databases with the highest Recall of 94.2%,
42 Precision of 95.6%, and F-score of 94.8% illustrate that the developed strategy outperforms the
43 state-of-the-art frameworks.

44 **Keywords:** Deep learning, Text detection, Curved texts, Convolutional neural networks, Text
45 segmentation.

46

47

48 **1. Introduction**

49 Automatically understanding of scene text with edges and corner-point information in a real
50 environment represent a significant influence in a diverse set of intelligent system applications in
51 visual assistance, intelligent traffic systems, automatic driving car, and so on [1]. In contrast to
52 algorithms based on the character or text applied to document images, which is sufficiently well
53 addressed by Optical Character Recognition (OCR) system, text classification and localization in
54 natural images are still an open complex problem [2]. Since text obtained from natural images
55 typically include a wide variety of useful text contents surrounded by objects in comparison to
56 graphics text, detecting target text in the real scene is a challenging task [3]. This is due to the fact
57 that the system needs to reject irrelevant objects and finds the location of the texts.

58 There are a number of weaknesses in a text localization system that work in only one direction
59 (horizontal), as a sizeable part of the texts achieved from natural images in the real world has a
60 wide range of orientations, sizes, and fonts [4]. Such restriction would make it fail to extract the
61 useful features contained in non-horizontal texts and thus seriously limits the efficiency and the
62 scalability of these strategies [5].

63 Usually, text detection strategies are based on two major algorithms: (i) approaches based on
64 the texture, and (ii) approaches based on the region [6]. The texture-based methods are based on
65 exploring significant features in the whole image, while the region-based techniques only work on
66 a part of the image to ease the problem of execution time [7]. The features in the region-based
67 techniques are permanently distinctive in real scene text regions [8]. The two main strategies for
68 doing this, are techniques based on the connected components and strategies based on the sliding
69 windows [5]. The CC strategies mostly emphasize significant information such as edges that can
70 be detected using an edge extracting algorithm or color-thresholding techniques and then

71 combining the sub-Maximally Stable Extremal Regions (MSER) parts into a text-line or word area
72 [9]. The mentioned strategies are capable to work in some hard detect scenarios including varying
73 brightness or contrast, light flickering, recognized stroke characters, display reflections, and
74 several joined characters. In the texture-based methods, by exploring the spreading of the textural
75 features in a local or global area, a surrounding window related to the text area can be easily chosen
76 and attached to text lines [10]. However, the significant disadvantages of strategies based on only
77 textures can be described by a simple feature extraction method. Techniques employing sliding
78 windows for feature extraction examine the image contents and try to extract numerous image
79 rectangles. Nevertheless, these methods lead to an increase in complexity and computational cost
80 [11].

81 The purpose of recognition of a wide range of texts is to identify and describe a sequence of
82 characters and content details from a selected region inside the text images for recognizing
83 signboards, license plates, and so on [12]. For recognizing the words, there is a need to detect them
84 first [1]. Due to the wide disparity in languages used in different areas and in dissimilar language
85 texts, significant parts of present scene text recognition approaches emphasize merely analyzing
86 the obtained image from the most applicable language texts (limited characters) [6]. To this end,
87 most of the text analyzing frameworks are widely investigated based on the English text and are
88 assorted into two key classes: the word-based and the character-based approaches [13]. Directly,
89 the word-based approach recognizes a similar pattern of the potential word inside the obtained
90 image from the real scene [14]. As countless English words are presented in the obtained real scene
91 images, common strategies cannot be able to determine a word or sentence directly without
92 needing to consider any extra information [15]. Basically, the character-based approach determines
93 all predefined characters inside a Region of Interest (ROI) by a character classifier. All extracted
94 characters make one or more words that can be recognized by a combination of individual
95 outcomes [16].

96 Recently, many Machine Learning (ML) methods are applied to various fields including
97 social sciences [17], optimization [18], regulatory systems [19], data augmentation [20], stochastic
98 systems [21], Internet of Medical Things [22], Internet of Things [23], Time series [24], medical
99 data analysis [25], degenerative disorder [26], and recommendation systems [27].

100 In recent years, to solve the problem and difficulty of text localization and detection in a real
101 scene due to the fuzzy boundary between text components and background, irregular shape, low

102 contrast, and low intensity numerous ML-based complex strategies have been implemented [28].
103 All segmentation and recognition algorithms are classified into two main groups based on
104 their characteristics, including semi-automatic techniques (interactive approaches) and automatic
105 frameworks [29]. The interactive or semi-automatic frameworks normally can be employed by
106 various Human-Machine Interactions (HMI) or user directions [30]. This kind of text detection is
107 somehow impossible to use in an environment that needs a real-time response [31]. So, automatic
108 frameworks have been employed in a number of applications to diminish the costs and time of
109 analyzing and steadily develop accuracy [32].

110 Current automatic models mainly can be explored inside the two wide-ranging classes,
111 including anti-learning and learning techniques [33]. The anti-learning frameworks regularly
112 comprise the active contour, clustering, region-growing, graph cut, and level set methods [34].
113 Region-growing approaches are pixel-based image segmentation strategies that select the touching
114 pixels iteratively with many similarities (homogeneities) in intensity, direction, color, or variance
115 (adding the neighboring pixels) [35]. The efficiency of region-growing algorithms can be
116 influenced by selecting the seed points, and they benefit from small calculation complexity and
117 high speed [36]. Graph cut methods are powerful energy minimization (optimization) strategies
118 that characterize the image to an undirected weighted graph. It means each input image can be
119 represented as a graph of nodes. Due to the use of both boundaries and regional information, it has
120 obtained a lot of attention [37]. In these approaches, there is a need to have prior information about
121 the shape and size of the target object, and every location (pixel) $p \in I$ inside the image is implied
122 as a node in the graph. Furthermore, every edge connects two adjacent nodes, therefore the weight
123 of each edge defines the rate of the similarities among each pair [38].

124 In recent years, employing a neuron-based model as an automatic learning approach such as
125 the Convolutional Neural Network (CNN/ConvNet) has been a surge of interest in text detection
126 in the real scene [39]. There are different kinds of neural networks (NNs) in deep learning, such
127 as artificial neural networks (ANN) [40], radial basis function (RBF) [41], convolutional neural
128 networks (CNN) [42], recurrent neural networks (RNN) [43], etc. Unlike hand-crafted feature
129 extraction models [44], these deep learning-based models are able to explore more informative
130 information and hidden pattern inside the input data automatically [34].

131 To overcome the problem of text instances with arbitrary shapes, Liu et al [16] proposed a
132 novel BezierAlign layer. The Bezier curve detection layer was employed to adaptively fit the

133 oriented or curved text. Ma et al. [45] proposed a combination of the Rotated Bounding Box
134 Representation method and Rotation Anchors technique to overcome the issues of text angle
135 information. They used the convolutional layers of VGG-16 as sharable layers for extracting the
136 low-level features, and the last convolutional layer is responsible for proposing the horizontal
137 region. Moreover, a multi-modal algorithm has been proposed by [46] for Bib text/number
138 recognition that is printed on cardboard tags or papers in Marathon natural images. This strategy
139 combines text detection and torso detection to obtain an acceptable result. As torso detection focus
140 on detecting the body parts such as the backside, stomach, and chest, there is no need to extract
141 features related to the face. By integrating the binarization process at the post-processing step for
142 segmenting texts, a Differentiable Binarization (DB) module is introduced in Liao et al. [47].
143 Moreover, they employed an efficient Adaptive Scale Fusion (ASF) module for improving the
144 robustness of scale variation by fusing features of diverse scales adaptively.

145 To address the issue of the complex background, a Scale-based Region Proposal Network has
146 been proposed by [48]. They investigated a two-stage pipeline to gain more accurate outcomes
147 along with faster detection speed to understand the content of the image rather than analyzing the
148 entire image. In the first stage, using a Scale-based Region Proposal Network, the location of the
149 text is estimated. Next, a Fully Convolutional Network (FCN) is implemented to attain an accurate
150 localization result. The described strategies suffer from intolerable outcomes in recognizing the
151 vertical text in the real scene, especially in the images with low illumination and low contrast
152 scenes. Also, these state-of-the-art techniques cannot properly identify the orientation and location
153 of the text efficiently. These problems lead to uncertainty in some applications such as blind
154 assistance systems and driver assistance systems. Therefore, to overcome these problems in this
155 study, a deep learning strategy is proposed to reduce the bad influence of the complex background
156 that is robust to variations in color, scale, and rotation. To address the problem of lacking color
157 information like Red, Green, and Blue (RGB), a multi-channel MSER technique was introduced
158 by [49]. Their model combined the enhanced multi-channel MSER focusing on the region and
159 Canny edge detector concentrating on the edge, where the channels employed in MSER consist of
160 B, G, and R channels of the RGB color space and the S channel of the Hue, Saturation, and
161 Intensity (HSI) color space.

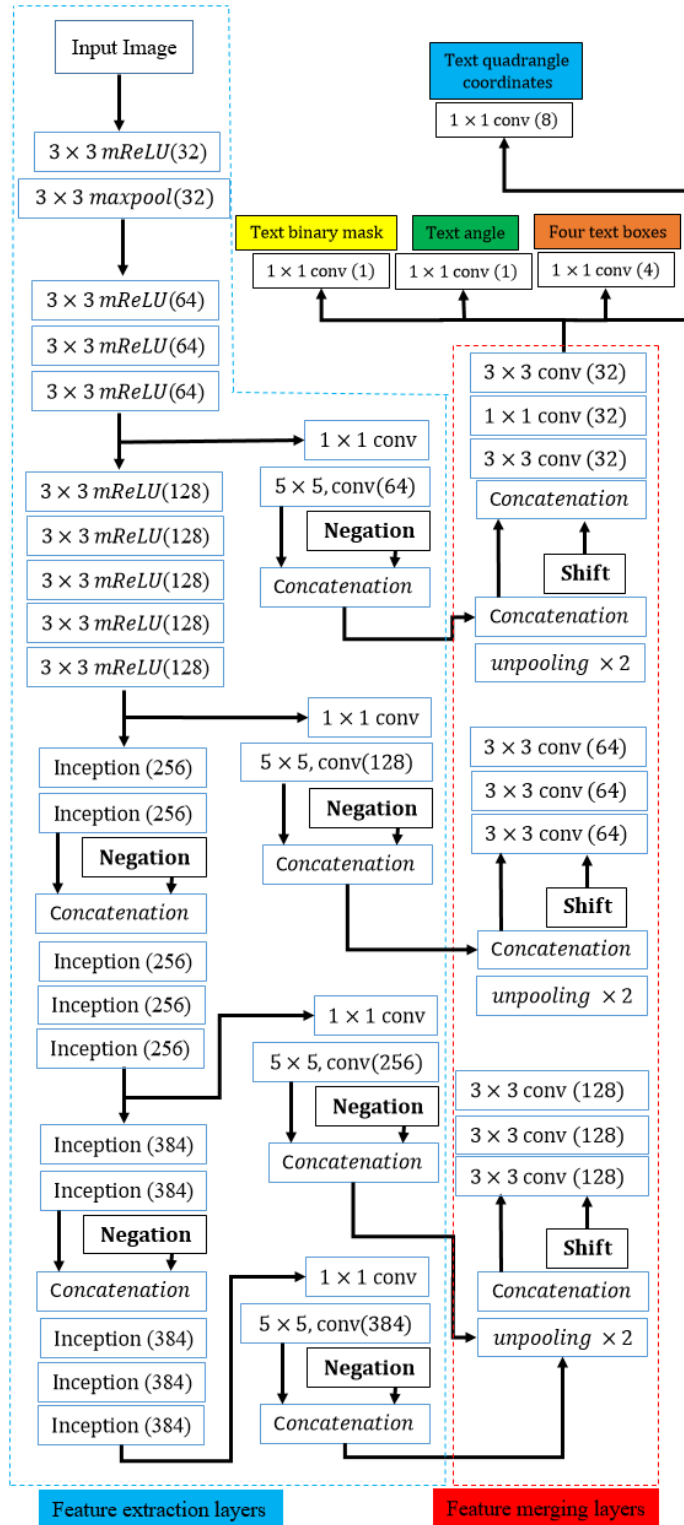
162 This study is structured as follows. In Section 2, the proposed methodology is described in
163 detail. In Section 3, the experiment results and comparison with some recently published pipelines

164 are investigated. Section 4 concludes the study and gives an outlook for future studies.

165 **2. Methodology**

166 In this study, a lightweight CNN architecture for text localization and detection is proposed
167 that aims to detect texts in the real scene, even if the text rotation is 90° . This contribution aims to
168 employ a convolutional neural network for localizing text more precisely. Moreover, some
169 intermediate time-consuming phases including word partitioning, finding the most possible region
170 of occurring, and text region formation are eliminated [50]. The proposed structure is demonstrated
171 in Fig. 1. The developed methodology in this research is capable to detect both the location and
172 rotation of the text and works well for the complex background. The structure of the combination
173 of the 3×3 *new.mReLU* block and the MaxPooling layer at the beginning of the network is used
174 for low-level visual feature extraction and plays a key role in the final results [50]. This network
175 for extracting mid-level and high-level features employs 5 *new.mReLU* blocks followed by 10
176 inception blocks. As shown in Fig. 2, the output of the final inception and *new.mReLU* blocks are
177 considered as the input of the four 1×1 Convolution Layers (Conv layers). These four
178 convolution layers and the next 5×5 convolution and negative layers aim to recognize the
179 vertical text.

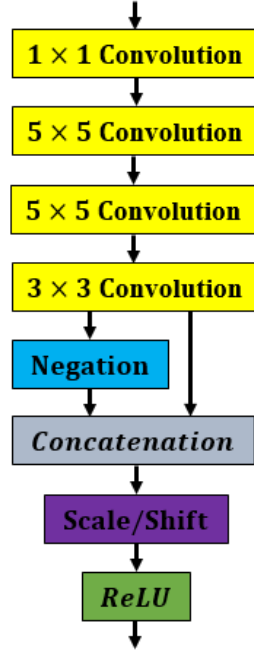
180 Furthermore, an additional layer is applied to increase the efficiency of the feature extraction.
181 Moreover, at the beginning of the proposed structure a new m.ReLU is utilized [51]. The
182 implemented 3×3 *new.mReLU* block is illustrated in Fig. 2. The intermediate activation
183 patterns in the CNNs are the main motivation for applying this module inside the proposed model
184 [52]. In this part, the production results obtained from the Negation and Conv layers need to be
185 concatenated [53]. Additionally, to ease the computational burden, a separated bias layer is applied
186 which causes the correlated kernels capable of having dissimilar bias weights.



187

188

Fig. 1. Proposed pipeline.



189

190

Fig. 2. Proposed 3×3 *new.mReLU* building block.

191

192

193

194

195

196

197

198

199

200

201

202

203

204

205

206

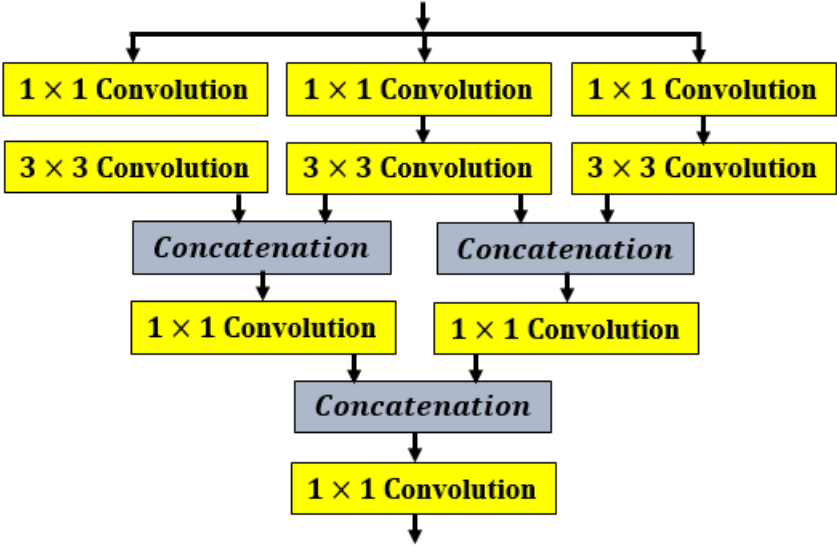
207

In the *new.mReLU* block, to overcome the limitation of the low contrast, the convolution output simply multiplies -1 by **Negation**. This Negation layer decreases the search space, compared to the recently published papers which predict four coordinates of an object [54]. Also, the trainable weights and biases can be applied to the next layer by **Scale/Shift** [55]. As the goal is to find a unique characteristic of text that can be determined for each text component at all levels, a **Scale/Shift** layer plays a key role in this purpose. It is also more dependable to estimate the rate of the text curvature to extract each character based on a distance ratio than identifying only a predefined distance between each character. To end this, the **Scale/Shift** layer needs to be after the concatenation layer. Using the *new.mReLU* layer allows us to extract some low-level features suitably and causes robustness to font distortion and variation. Moreover, to address the issue of the complex background, three sequences of this layer at the beginning of the network have been employed [56].

A crucial step for achieving significant text detection results is exploring all potential areas inside the image including different scales, colors, and sizes [57]. It should be mentioned that extracted information from the different colorful textures plays a core role in improving the feature extraction procedure. This is because of intense color similarity in the most of characters and texts in the natural scene text (like warning traffic sign boards). Consequently, the proposed inception

208 block is represented for improving the localization of the multi-scale and multi-orientation texts
 209 and preventing the production of more false-positive rates [55]. The proposed inception pipeline
 210 can be observed in Fig. 3.

211 Our new inception block is inspired by some of the suggestions implemented in Szegedy et
 212 al. [58] and comprises three parallel convolutional networks at the first, and one sequential
 213 concatenation and convolutional layers at the end of the block [59]. The core idea applied by the
 214 inception pipeline is eliminating the Conv layer and employing various parallel architectures to
 215 cover a larger region whereas a fine resolution can be obtained [60]. This approach forces
 216 multiplicity on the obtained features from each layer by merging feature maps at the end of the
 217 inception block and indicating a diminishing rate in the number of parameters. By overcoming the
 218 problems of changing the size of the text font employing this block, the accuracy of the final system
 219 output has successfully been improved. Here, it is realized that to attain an improvement in
 220 detecting largely varying-sized text, using stacking up inception layers is further useful than a
 221 simple linear chain of Conv layers [61]. Besides, to make the system more powerful to explore the
 222 location of the text with the minimum number of parameters the size of receptive fields is altered.
 223 Additionally, to ease the computational burden, two concatenation steps after extracting features
 224 in 3×3 Conv layers were employed.



225
 226 **Fig. 3.** Suggested inception building block.

227 As indicated in Fig. 1, stacking up inception layers are able to detect more varying-sized texts
 228 in an effective way compared to a chain of Conv layers. Owing to the use of the suggested

229 inception building block, the output feature maps are produced with the same dimension of
 230 receptive fields. The output of the proposed structure can be implied as four detached vectors of
 231 features (both 1D and 2D vectors). The first feature vector is a 2D binary matrix (binary image)
 232 that is generated by considering the value of one for pixels inside the text window whereas others
 233 are represented by zero values. The next output vector is defined as the rotation of the text. The
 234 third output feature maps naming R matrices are represented by four **axis-aligned bounding boxes**
 235 (AABB). These output feature maps (2D vectors) can be considered as the distance of pixels to
 236 four corners of the obtained window that is fitted to the outer profile of the text [14]. Lastly, eight
 237 1D vectors are generated to imply the corners of the text box's location (four corners) in the y and
 238 x directions. It means each corner can be defined by two distance variables: dx and dy . Then, the
 239 rotation map of text (rotation of each character) is calculated inside the described box with
 240 acceptable accuracy and demonstrated in a grayscale image. In order to attain the corners of the
 241 text box's location (eight channels), $LOC = \{p_i | i \in \{1,2,3,4\}\}$ is taken into account, where these
 242 vertices are defined by $p_i = \{x_i, y_j\}$. Besides, the reference length ref_i can be calculated for each
 243 vertex p_i as:

$$ref_i = \min \left(dist(p_i, p_{(i \bmod 4)+1}), dist(p_i, p_{((i+3) \bmod 4)+1}) \right), \quad (1)$$

244 where $dist(p_i, p_j)$ represents the Euclidean distance between p_j and p_i .

245 This binary mask (score map) can be produced by applying shrinking on each edge of the box
 246 by $0.38 \times ref_i$ and $0.38 \times ref_{(i \bmod 4)+1}$. In other words, to fit the obtained window around the
 247 text, the distances between these obtained 8 indices (or 8 channels) and 8 corners of the text inside
 248 the scene should be minimized. Hence, the value of 0.4 was chosen based on many experiments.

249 The loss function for text detection can be formulated as:

$$Loss_{total} = loss_{Score\ map} + \lambda_{Geometry} Loss_{Geometry}, \quad (2)$$

250 where $loss_{Score\ map}$ (oriented class-balanced cross-entropy) indicates the losses for the score map
 251 and $Loss_{Geometry}$ indicates the losses geometry. Moreover, $\lambda_{Geometry}$ implies the balancing
 252 weights t between two losses for achieving more robustness and accuracy.

253 The oriented class-balanced cross-entropy for minimizing the loss of score map is calculated
 254 using Equation (3):

$$loss_{Score\ map} = \zeta out_{reference} \log out_{predicted} - (1 - \zeta)(1 - out_{reference}) \log(1 - out_{predicted}), \quad (3)$$

255 where ζ indicates the oriented text balancing factor between negative and positive samples, given
256 by Equation (4):

$$\zeta = \left(\frac{\sum_{corners \in out_{reference}(i)} corners - \sum_{corners \in out_{reference}(i+1)} corners}{\sum_{corners \in out_{predicted}(i)} corners - \sum_{corners \in out_{predicted}(i+1)} corners} \right) \times \left(1 - \frac{\sum_{T \in out_{reference}} T}{|out_{reference}|} \right) \quad (4)$$

257 where i represents the current detected text and $i + 1$ demonstrates the adjacent detected text as
258 shown in Fig. 4.

259 By considering the effect of distances between the current detected text and the adjacent
260 detected text, the suggested network is able to predict the rotation of the text more efficiently. In
261 this study, $\lambda_{Geometry}$ is set to 0.83 and the proposed structure was learned in 1,000 epochs with a
262 batch size of 128, a learning rate of 0.01, and a weight decay of 0.0001. Furthermore, $Loss_{Geometry}$
263 can be described as:

$$Loss_{Geometry} = \alpha_{\theta} loss_{\theta} + Loss_{AABB}, \quad (5)$$

$$Loss_{AABB} = -\log \left(\frac{|reference \cap predicted|}{|reference \cup predicted|} \right), \quad (6)$$

264 where $predicted$ shows the calculated AABB geometry and $reference$ is the related Ground
265 Truth (GT). Furthermore, by defining $dis_1, dis_2, dis_3,$ and dis_4 as the distance from a pixel to the
266 bottom, left, top, and right boundary of its corresponding window, the height and width of the
267 intersected rectangle $|reference \cap predicted|$ are calculated using Equations (7) and (8):

$$width = \min(dis_2(reference), dis_2(predicted)) + \min(dis_4(reference), dis_4(predicted)), \quad (7)$$

$$height = \min(dis_1(reference), dis_1(predicted)) + \min(dis_3(reference), dis_3(predicted)). \quad (8)$$

268 Moreover, the union region can be calculated by Equation (9):

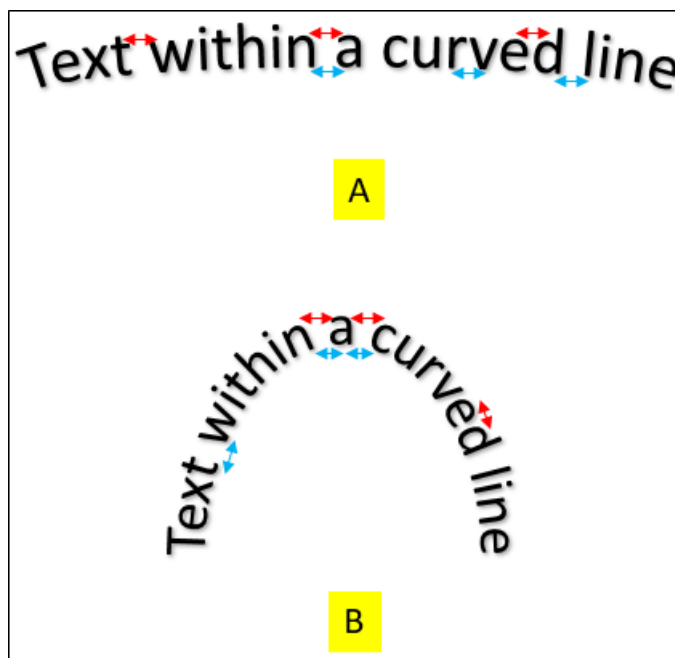
$$|reference \cup predicted| = |reference| + |predicted| - |reference \cap predicted|. \quad (9)$$

269 Then, the loss function of rotation angle is given by Equation (10):

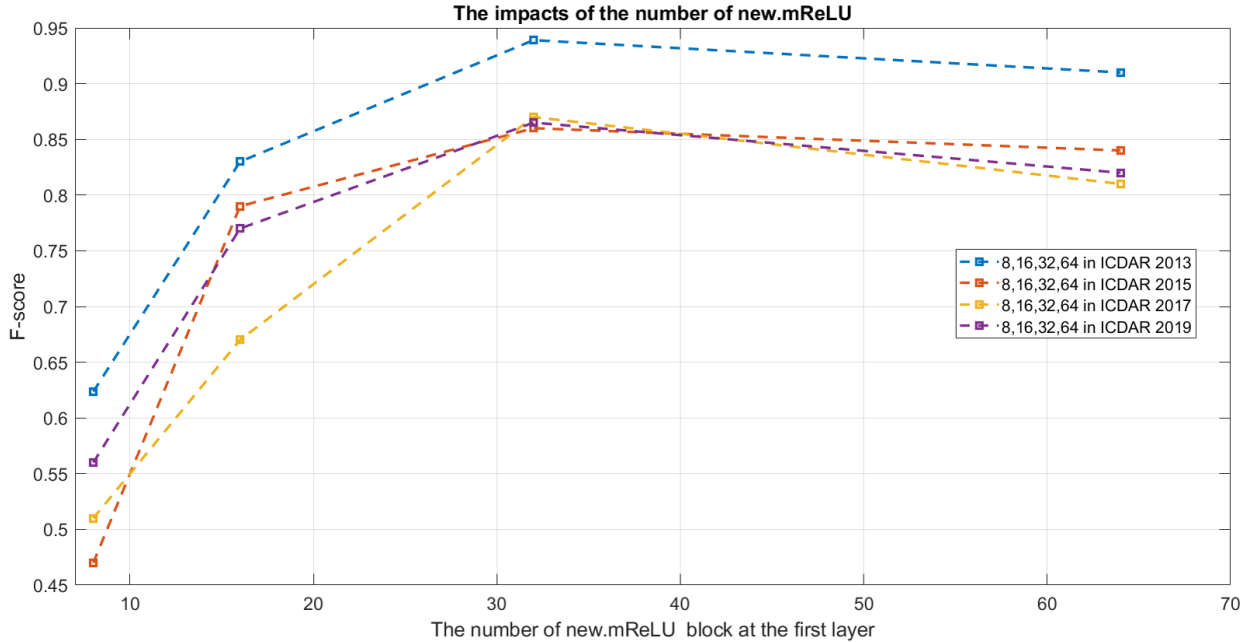
$$L_{\theta}(\theta_{predicted}, \theta_{reference}) = 1 - \cos(\theta_{predicted} - \theta_{reference}). \quad (10)$$

270 Furthermore, it is identified that using only a 3×3 convolution layer after up-sampling and
271 concatenation layers (see Fig. 1) causes a difficulty to precisely recognize the horizontal sides of
272 words in the case of observing text on a curve. This is due to the fact that the distance of each

273 character to the adjacent character is uneven for the upper and bottom parts of it which changes
274 the shape of the components. In other words, as it is illustrated in Fig. 4, within a word in a curved
275 line, it is a confusing task to find the exact distance between each character. Moreover, whatever
276 the two borders of the text are closer together (see Fig. 4 (B)) the distance between the upper parts
277 of the words or characters is bigger and vice versa. To overcome this problem, two 3×3
278 convolution layers have been utilized after the up-pooling and concatenation layers. Furthermore,
279 as mentioned before, the first *new.mReLU* layers are crucial for obtaining acceptable results.
280 Hence, the impacts of the number of this layer are demonstrated in Fig. 5.



281
282 **Fig. 4.** Two examples of observing text in the real scene. (A) A sample text with a small curvature. (B) A
283 sample text with high curvature. The red arrows indicate a bigger distance than the blue arrows. As it is
284 clearly demonstrated the red arrows inside the (B) are bigger than the blue arrows, whilst these arrows are
285 small differences in (A).



286

287

Fig. 5. Impacts of the number of the *new.mReLU* blocks on all tested datasets.

288

3. Experiments

289

3.1 Datasets

290

291

292

293

294

295

296

297

298

In order to assess the proposed method, the datasets of ICDAR 2013 [62], ICDAR 2015 [63], ICDAR 2017 [64], and ICDAR 2019 [65] are utilized. They have been cited and used by several recent scene text research works. The ICDAR 2013 is based on the horizontal text which includes 229 and 223 images for training and testing, respectively. Also, the ICDAR 2015 is based on multi-oriented text with 1000 and 500 images for training and testing, respectively [56]. Moreover, the ICDAR 2017 consists of 1555 images with various text orientations. Finally, the ICDAR 2019 consists of 10,000 images for robust text locating [66]. Text detection results are illustrated in Figs. 6, 7, 8, and 9. It has been illustrated that text orientation and location can be successfully detected by the suggested algorithm.

299

3.2 Evaluation metrics

300

301

302

In this study, the following three measures, namely f-measure (F), recall (R), and precision (P), have been used to evaluate the developed model and compare the text detection results with some state-of-the-art approaches. These metrics can be defined as follows [67]:

$$\text{Precision} = \frac{TP}{TP + FP}, \quad (11)$$

$$\text{Recall} = \frac{TP}{TP + FN}, \quad (12)$$

$$F = \frac{2 \times \text{Precision} \times \text{Recall}}{\text{Precision} + \text{Recall}}, \quad (13)$$

303 where the FN , FP , and TP respectively represent the false negative, false positive, and true positive
 304 [68]. The outstanding results and experiments were accomplished utilizing Python on an Intel 3.2
 305 GHz-Core I7 computer with a 64-bit operating system.

306 **3.3 Experimental Results**

307 In order to verify the performance and robustness of the suggested approach, it is compared
 308 with 10 state-of-the-art text localization pipelines. For a more clear understanding, vertical text
 309 localization is depicted in Fig. 8. Due to the trade-off between recall and precision result rate, the
 310 f-score is the best evaluation for analyzing the results of a text detection system. The outcomes are
 311 described and compared with the other pipelines in Tables 1-4. For each index in all tables, the
 312 highest values are highlighted in bold. By analyzing the indicated outcomes in Tables 1-4, it is
 313 obvious that the proposed pipeline has gained the best outcomes in comparison with all mentioned
 314 detection architectures. The notable obtained outcomes prove that the given strategy meaningfully
 315 improves the accuracy of the model even with the presence of texts with 90° orientation in the
 316 scene. Furthermore, to exemplify the importance of implementing the proposed network to
 317 accurately estimate the text location, Figs. 6-9 demonstrate the outcomes of the offered structure.

318 The effectiveness and accuracy of the proposed strategy are first investigated on a popular
 319 horizontal text dataset, namely the ICDAR 2013 dataset. As clearly shown in Table 1, the proposed
 320 pipeline obtains competitive performance both in terms of efficiency and accuracy. Although the
 321 CRAFT [15] and achieves the highest precision, the highest Recall and F-measure are obtained by
 322 the proposed methods. The Recall of TextBox MS [69] is only next to LocNet [57] and SRPN
 323 [48]. Moreover, Fast TextBox [69] obtains the worst results in all three measures. Examples of
 324 text detection on the ICDAR 2013 dataset are illustrated in Fig. 6.

325
 326
 327
 328

Table 1. Results on ICDAR 2013.

Method	Recall	Precision	F-score
AF-RPN [70]	0.900	0.934	0.916
FTPN [5]	0.919	0.932	0.925
TextBox MS [69]	0.830	0.880	0.850
Fast TextBox [69]	0.740	0.860	0.800
Pyramid Context Network [28]	0.905	0.938	0.921
DeRPN [71]	0.774	0.867	0.818
LocNet [57]	0.875	0.940	0.906
CRAFT [15]	0.931	0.974	0.952
Delaunay Triangulation (DT) [72]	0.904	0.88	0.891
SRPN [48]	0.842	0.925	0.882
Multi-channel MSER [49]	0.937	0.894	0.915
The proposed approach	0.942	0.956	0.948

330



331

332 **Fig. 6.** Example of four text localization by the proposed method on ICDAR 2013. It is shown that the
 333 proposed method is capable of localizing the oriented text successfully.

334 By analyzing the outcomes achieved on ICDAR 2015 in [Table 2](#), it is found out that there is
 335 not much difference between the minimum and maximum values based on the Recall criteria.
 336 Accordingly, it can noticeably be seen that the worst scores for Precision and Recall were obtained
 337 using EAST+VGG16 [14] and SegLink [73], respectively. Results obtained using
 338 PixelLink+VGG16 4s [12] and PixelLink+VGG16 2s [12] are very close to the proposed network

339 regarding the Recall; however, it still failed to detect words as the Precision score
 340 demonstrates. Deep Direct Regression [4] and SegLink [73] methods cannot gain acceptable
 341 results, especially in the presence of a complex background. PixelLink+VGG16 2s [12], Multi-
 342 channel MSER [49], PixelLink+VGG16 4s [12], and Mask R-CNN [74] approaches are good to
 343 extract the oriented text when there is much similarity between two completely separated words,
 344 whilst they perform so poorly when encountering two close words. Moreover, EAST+PVANET2x
 345 MS [14] and EAST+PVANET2x [14] models are more prone to fail, especially when there are
 346 fuzzy boundaries. Finally, the developed approach reaches the best performance with the ICDAR
 347 2015 dataset, followed by Mask R-CNN [74] which has a small difference in Precision score. Fig.
 348 7 depicts that the suggested model has a powerful ability to detect curved texts. It is even able to
 349 read words within a short distance.

350

351

Table 2. Results on ICDAR 2015.

Method	Recall	Precision	F-score
EAST+VGG16 [14]	0.727	0.804	0.764
EAST+PVANET2x [14]	0.734	0.835	0.782
EAST+PVANET2x MS [14]	0.7563	0.7712	0.7516
SegLink [73]	0.768	0.731	0.750
Mask R-CNN [74]	0.815	0.908	0.859
Deep Direct Regression [4]	0.800	0.820	0.810
PixelLink+VGG16 4s [12]	0.817	0.829	0.823
PixelLink+VGG16 2s [12]	0.820	0.855	0.837
Direct Regression [2]	0.800	0.850	0.820
SRPN [48]	0.796	0.920	0.853
Adaptive scale fusion [47]	0.839	0.909	0.873
Kernel Proposal Network [75]	0.869	0.878	0.873
Multi-channel MSER [49]	0.922	0.894	0.903
The proposed approach	0.931	0.924	0.927

352



353

354 **Fig. 7.** Example of four text localization by the suggested method on ICDAR 2015. It is shown that the
355 proposed method is capable of localizing the oriented text successfully.

356 As indicated in [Table 3](#), text detection and segmentation by employing AF-RPN [70] and
357 CLRS [76] imply the fewest match with the ground truth, especially when there are vertical texts.
358 This is due to the fact that the vertical and horizontal texts exhibit different characteristics.
359 Moreover, PSENet [77] obtains the worst Precision score amongst all evaluated approaches.
360 Compared with previous state-of-the-art pipelines in the field of text localization, the developed
361 pipeline in this work demonstrates the advantage in terms of Recall, Precision, and F-score.
362 Delaunay Triangulation outperformed Mask R-CNN [74] and reached competitive outcomes
363 against state-of-the-art algorithms (AF-RPN, PSENet, TSL, and ISNet). AF-RPN [70] and ISNet
364 [78] models had issues identifying vertical word cases and when it does, they were detected with
365 a very low confidence value. Delaunay Triangulation method [72] was very close to the developed
366 approach regarding the Recall; however, it still failed to detect words as the Precision score
367 demonstrates. [Fig. 8](#) depicts that the suggested model has a powerful ability to detect curved texts.
368 It is even able to read words within a short distance.

369

370

371

372

373

374

Table 3. Results on ICDAR 2017.

Method	Recall	Precision	F-score
AF-RPN [70]	0.667	0.794	0.725
PSENet [77]	0.753	0.691	0.721
TSL [79]	0.674	0.776	0.722
Delaunay Triangulation (DT) [72]	0.83	0.72	0.771
ISNet [78]	0.674	0.78	0.723
CLRS [76]	0.556	0.838	0.668
Mask R-CNN [74]	0.698	0.8	0.743
Multi-channel MSER [49]	0.806	0.764	0.784
The proposed approach	0.874	0.867	0.870

375

376



377

Fig. 8. Example of four text localization by the suggested method on ICDAR 2017. It is shown that the proposed method is capable of localizing the vertical and curved texts magnificently.

380

381 Experimental outcomes on the ICDAR 2019 illustrate that the developed pipeline
 382 outperformed well-known techniques, such as LOMO [80], Pyramid Context Network [28], and
 383 PixelLink+VGG16 2s [14] not only in effectiveness and accuracy but also in terms of the size of
 384 the network. As indicated in Table 4, text identification by applying Fast TextBox [69],
 385 EAST+PVANET2x [14], and TextBox MS [69] entails the fewest match with the ground truth,

386 especially when there are vertical texts. From the obtained outcomes and Fig. 9, it can be observed
 387 that the identification is able to automatically be adapted to any kind of text, even with the different
 388 distances between characters. Concerning the best structures for detecting a text and their networks
 389 dimension, PixelLink+VGG16 2s [12], PixelLink+VGG16 4s [12], and Pyramid Context Network
 390 [28] achieved better results than Fast TextBox [69] and EAST+PVANET2x [14]; nevertheless,
 391 their models were larger than the proposed network. On the whole, the experimental outcomes
 392 imply the superiority of the developed approach.

393

394

Table 4. Results on ICDAR 2019.

Method	Recall	Precision	F-score
LOMO [80]	0.798	0.878	0.836
EAST+PVANET2x [14]	0.751	0.816	0.782
TextBox MS [69]	0.775	0.884	0.825
Fast TextBox [69]	0.753	0.845	0.796
Pyramid Context Network [28]	0.815	0.846	0.830
PixelLink+VGG16 4s [12]	0.823	0.821	0.821
PixelLink+VGG16 2s [12]	0.820	0.855	0.837
The proposed approach	0.842	0.891	0.865

395

396



397

398 **Fig. 9.** Example of four text localization by the suggested method on ICDAR 2019. It is shown that the
 399 proposed method is capable of localizing the oriented texts magnificently.

400

401 DL-based techniques have a key drawback that it is challenging for determining the basis of
 402 the proposed network judgment. The common technique to clarify the reason for the model
 403 prediction is visual description. The visual description technique illustrates an attention map that
 404 pictures an area in which the model concentrated as a heat map [81]. According to an achieved

405 attention map, the reason for the segmentation or classification results can be understood and
406 analyzed. In order to gain a clearer and more explainable attention map for a well-organized visual
407 description, a number of techniques such as Class Activation Mapping (CAM) and Gradient-
408 weighted Class Activation Mapping (Grad-CAM) have been suggested in the field of computer
409 vision [82].

410 In this study, the Grad-CAM method produces an attention map by utilizing gradient values
411 computed at the backpropagation process. Fig. 10 illustrates example attention maps of Grad-
412 CAM.

413



414

415 **Fig. 10.** Two examples of Grad-CAM of the suggested network. The first row and the second row indicate
416 the original and Grad-CAM images, respectively. Color denotes the degree of activation: very low (blue),
417 low (green), high (yellow) and very high (red).

418

419 4. Conclusion

420 In this research, a new real scene text detection pipeline was implemented based on an
421 inception structure that can produce a location binary mask along with its rotation. The proposed
422 structure overcame some problems such as local and global illumination variations, occlusion, a
423 wide range of styles and colors, unpredictable orientations, and various sizes. This strategy was
424 also capable of discovering even vertical texts in a real scene. By incorporating an extra layer for
425 feature extraction and an optimized inception layer, the detector can find the text location more
426 accurately.

427 Our structure was based on the combination of the *new.mReLU* and inception structure.
428 Because of utilizing *new.mReLU* and inception blocks, text recognition also can be implemented
429 more precisely and efficiently. Experimental comparisons with the state-of-the-art structures on
430 four datasets; ICDAR2013, ICDAR2015, ICDAR2017, and ICDAR2019 depicted the efficiency
431 and effectiveness of the developed approach for the text localization and recognition task. Each of
432 these datasets is recorded in different environments with various image resolutions and light
433 conditions. As there are some restrictions for detecting text in the presence of a complex
434 background, the most important idea to extend this study is to use a transform learning approach
435 for increasing the accuracy of the developed approach.

436
437 **Funding** This publication has emanated from research [conducted with the financial support
438 of/supported in part by a grant from Science Foundation Ireland under Grant number No.
439 18/CRT/6183 and is supported by the ADAPT Centre for Digital Content Technology which is
440 funded under the SFI Research Centres Programme (Grant 13/RC/2106/_P2), Lero SFI Centre for
441 Software (Grant 13/RC/2094/_P2) and is co-funded under the European Regional Development
442 Fund. For the purpose of Open Access, the author has applied a CC BY public copyright license
443 to any Author Accepted Manuscript version arising from this submission.

444 **Declarations Ethics Approval** This article does not contain any studies with human participants
445 or animals performed by any of the authors.

446 **Informed Consent** Not applicable.

447 **Conflict of Interest** The authors declare that they have no conflict of interest regarding this work.

448 **References**

- 449 [1] S. Y. Arafat, N. Ashraf, M. J. Iqbal, I. Ahmad, S. Khan, and J. J. P. C. Rodrigues, “Urdu
450 signboard detection and recognition using deep learning,” *Multimed. Tools Appl.*, vol. 81,
451 no. 9, pp. 11965–11987, Apr. 2022, doi: 10.1007/S11042-020-10175-2/FIGURES/14.
- 452 [2] W. He, X. Y. Zhang, F. Yin, and C. L. Liu, “Multi-Oriented and Multi-Lingual Scene Text
453 Detection with Direct Regression,” *IEEE Trans. Image Process.*, vol. 27, no. 11, pp. 5406–
454 5419, Nov. 2018, doi: 10.1109/TIP.2018.2855399.
- 455 [3] A. Aiman, Y. Shen, M. Bendeche, I. Inayat, and T. Kumar, “AUDD: Audio Urdu Digits
456 Dataset for Automatic Audio Urdu Digit Recognition,” *Appl. Sci.* 2021, Vol. 11, Page 8842,
457 vol. 11, no. 19, p. 8842, Sep. 2021, doi: 10.3390/APP11198842.
- 458 [4] W. He, X.-Y. Zhang, F. Yin, and C.-L. Liu, “Deep Direct Regression for Multi-Oriented
459 Scene Text Detection,” 2017.
- 460 [5] F. Liu, C. Chen, D. Gu, and J. Zheng, “FTPN: Scene text detection with feature pyramid
461 based text proposal network,” *IEEE Access*, vol. 7, pp. 44219–44228, 2019, doi:
462 10.1109/ACCESS.2019.2908933.
- 463 [6] G. Jawahar, M. Abdul-Mageed, and L. V. S. Lakshmanan, “Automatic Detection of
464 Machine Generated Text: A Critical Survey,” Nov. 2020, Accessed: Dec. 26, 2020.
465 [Online]. Available: <http://arxiv.org/abs/2011.01314>.
- 466 [7] N. Tataei Sarshar et al., “Glioma Brain Tumor Segmentation in Four MRI Modalities Using
467 a Convolutional Neural Network and Based on a Transfer Learning Method,” pp. 386–402,
468 2023, doi: 10.1007/978-3-031-04435-9_39.
- 469 [8] W. ; Khan et al., “Introducing Urdu Digits Dataset with Demonstration of an Efficient and
470 Robust Noisy Decoder-Based Pseudo Example Generator,” *Symmetry* 2022, Vol. 14, Page
471 1976, vol. 14, no. 10, p. 1976, Sep. 2022, doi: 10.3390/SYM14101976.
- 472 [9] L. Zou, Z. Wang, and D. Zhou, “Moving horizon estimation with non-uniform sampling
473 under component-based dynamic event-triggered transmission,” *Automatica*, vol. 120, p.
474 109154, Oct. 2020, doi: 10.1016/j.automatica.2020.109154.

- 475 [10] R. Ranjbarzadeh and S. Baseri Saadi, “Corrigendum to ‘Automated liver and tumor
476 segmentation based on concave and convex points using fuzzy c-means and mean shift
477 clustering’ [Measurement 150 (2020) 107086],” *Measurement*, vol. 151, p. 107230, Feb.
478 2020, doi: 10.1016/J.MEASUREMENT.2019.107230.
- 479 [11] S. Long, X. He, and C. Yao, “Scene Text Detection and Recognition: The Deep Learning
480 Era,” *Int. J. Comput. Vis.*, pp. 1–24, Aug. 2020, doi: 10.1007/s11263-020-01369-0.
- 481 [12] D. Deng, H. Liu, X. Li, and D. Cai, “PixelLink: Detecting Scene Text via Instance
482 Segmentation,” *32nd AAAI Conf. Artif. Intell. AAAI 2018*, pp. 6773–6780, Jan. 2018,
483 Accessed: Dec. 24, 2020. [Online]. Available: <http://arxiv.org/abs/1801.01315>.
- 484 [13] X. Bian, C. Wang, W. Quan, J. Ye, X. Zhang, and D. M. Yan, “Scene text removal via
485 cascaded text stroke detection and erasing,” *Comput. Vis. Media* 2021 82, vol. 8, no. 2, pp.
486 273–287, Dec. 2021, doi: 10.1007/S41095-021-0242-8.
- 487 [14] X. Zhou et al., “EAST: An Efficient and Accurate Scene Text Detector,” 2017.
- 488 [15] Y. Baek, B. Lee, D. Han, S. Yun, and H. Lee, “Character Region Awareness for Text
489 Detection,” 2019.
- 490 [16] Y. Liu, H. Chen, C. Shen, T. He, L. Jin, and L. Wang, “ABCNet: Real-time Scene Text
491 Spotting with Adaptive Bezier-Curve Network *,” 2020.
- 492 [17] E. Kropat, G.-W. Weber, and E. B. Tirkolaee, “Foundations of semialgebraic gene-
493 environment networks,” *J. Dyn. Games*. 2020, Vol. 7, Pages 253-268, vol. 7, no. 4, p. 253,
494 Jul. 2020, doi: 10.3934/JDG.2020018.
- 495 [18] A. Özmen, E. Kropat, and G. W. Weber, “Robust optimization in spline regression models
496 for multi-model regulatory networks under polyhedral uncertainty,” vol. 66, no. 12, pp.
497 2135–2155, Dec. 2016, doi: 10.1080/02331934.2016.1209672.
- 498 [19] E. Kropat, A. Ozmen, G. W. Weber, S. Meyer-Nieberg, and O. Defterli, “Fuzzy prediction
499 strategies for gene-environment networks – Fuzzy regression analysis for two-modal
500 regulatory systems,” *RAIRO - Oper. Res.*, vol. 50, no. 2, pp. 413–435, Apr. 2016, doi:
501 10.1051/RO/2015044.

- 502 [20] T. J. S.-H. Kumar, “Intra-Class Random Erasing (ICRE) augmentation for audio
503 classification,” Proc. Korean Soc. Broadcast Eng. Conf., pp. 244–247, 2020.
- 504 [21] B. Kalaycı, A. Özmen, and G. W. Weber, “Mutual relevance of investor sentiment and
505 finance by modeling coupled stochastic systems with MARS,” Ann. Oper. Res., vol. 295,
506 no. 1, pp. 183–206, Dec. 2020, doi: 10.1007/S10479-020-03757-8/TABLES/1.
- 507 [22] I. A. Khan et al., “XSRU-IoMT: Explainable simple recurrent units for threat detection in
508 Internet of Medical Things networks,” Futur. Gener. Comput. Syst., vol. 127, pp. 181–193,
509 Feb. 2022, doi: 10.1016/J.FUTURE.2021.09.010.
- 510 [23] A. K. Sahu, S. Sharma, M. Tanveer, and R. Raja, “Internet of Things attack detection using
511 hybrid Deep Learning Model,” Comput. Commun., vol. 176, pp. 146–154, Aug. 2021, doi:
512 10.1016/J.COMCOM.2021.05.024.
- 513 [24] Z. Yue et al., “Privacy-preserving Time-series Medical Images Analysis Using a Hybrid
514 Deep Learning Framework,” ACM Trans. Internet Technol., vol. 21, no. 3, Jun. 2021, doi:
515 10.1145/3383779.
- 516 [25] R. Sharma, T. Goel, M. Tanveer, and R. Murugan, “FDN-ADNet: Fuzzy LS-TWSVM
517 based deep learning network for prognosis of the Alzheimer’s disease using the sagittal
518 plane of MRI scans,” Appl. Soft Comput., vol. 115, p. 108099, Jan. 2022, doi:
519 10.1016/J.ASOC.2021.108099.
- 520 [26] S. Dwivedi, T. Goel, M. Tanveer, R. Murugan, and R. Sharma, “Multimodal Fusion-Based
521 Deep Learning Network for Effective Diagnosis of Alzheimer’s Disease,” IEEE Multimed.,
522 vol. 29, no. 2, pp. 45–55, 2022, doi: 10.1109/MMUL.2022.3156471.
- 523 [27] A. Chakraborty, D. Ganguly, A. Caputo, and G. J. F. Jones, “Kernel Density Estimation
524 based Factored Relevance Model for Multi-Contextual Point-of-Interest Recommendation,”
525 Inf. Retr. J., vol. 25, no. 1, pp. 44–90, Jun. 2020, doi: 10.48550/arxiv.2006.15679.
- 526 [28] E. Xie, Y. Zang, S. Shao, G. Yu, C. Yao, and G. Li, “Scene text detection with supervised
527 pyramid context network,” in 33rd AAAI Conference on Artificial Intelligence, AAAI
528 2019, 31st Innovative Applications of Artificial Intelligence Conference, IAAI 2019 and
529 the 9th AAAI Symposium on Educational Advances in Artificial Intelligence, EAAI 2019,

- 530 Jul. 2019, vol. 33, no. 01, pp. 9038–9045, doi: 10.1609/aaai.v33i01.33019038.
- 531 [29] A. Baghban, M. Bahadori, A. S. Lemraski, and A. Bahadori, “Prediction of solubility of
532 ammonia in liquid electrolytes using Least Square Support Vector Machines,” *Ain Shams*
533 *Eng. J.*, vol. 9, no. 4, pp. 1303–1312, Dec. 2018, doi: 10.1016/J.ASEJ.2016.08.006.
- 534 [30] Z. Liu and A. Baghban, “Application of LSSVM for biodiesel production using supercritical
535 ethanol solvent,” vol. 39, no. 17, pp. 1869–1874, Oct. 2017, doi:
536 10.1080/15567036.2017.1380732.
- 537 [31] M. T. S. T. R. B. and M. B. Teerath Kumar et al., “Forged Character Detection Datasets:
538 Passports, Driving Licences and Visa Stickers,” *Int. Artif. Appl. Vol.13,No.2*, vol. 13, no.
539 2, p. 21, Mar. 2022, doi: 10.5121/IJAIA.2022.13202.
- 540 [32] B. Du, J. Ye, J. Zhang, J. Liu, and D. Tao, “I3CL: Intra- and Inter-Instance Collaborative
541 Learning for Arbitrary-Shaped Scene Text Detection,” *Int. J. Comput. Vis.*, vol. 130, no. 8,
542 pp. 1961–1977, Aug. 2022, doi: 10.1007/S11263-022-01616-6/FIGURES/11.
- 543 [33] T. Kumar, J. Park, M. S. Ali, A. F. M. Shahab Uddin, J. H. Ko, and S.-H. Bae, “Binary-
544 Classifiers-Enabled Filters for Semi-Supervised Learning,” *IEEE Access*, pp. 1–1, 2021,
545 doi: 10.1109/ACCESS.2021.3124200.
- 546 [34] R. Ranjbarzadeh et al., “Nerve optic segmentation in CT images using a deep learning
547 model and a texture descriptor,” *Complex Intell. Syst.* 2022, pp. 1–15, Feb. 2022, doi:
548 10.1007/S40747-022-00694-W.
- 549 [35] R. Ranjbarzadeh et al., “MRFE-CNN: multi-route feature extraction model for breast tumor
550 segmentation in Mammograms using a convolutional neural network,” *Ann. Oper. Res.*
551 2022, pp. 1–22, May 2022, doi: 10.1007/S10479-022-04755-8.
- 552 [36] A. Aghamohammadi, R. Ranjbarzadeh, F. Naiemi, M. Mogharrebi, S. Dorosti, and M.
553 Bendeche, “TPCNN: Two-path convolutional neural network for tumor and liver
554 segmentation in CT images using a novel encoding approach,” *Expert Syst. Appl.*, vol. 183,
555 p. 115406, Nov. 2021, doi: 10.1016/J.ESWA.2021.115406.
- 556 [37] X. Liu and W. Wang, “An effective graph-cut scene text localization with embedded text
557 segmentation,” *Multimed. Tools Appl.*, vol. 74, no. 13, pp. 4891–4906, Jun. 2015, doi:

- 558 10.1007/s11042-013-1848-3.
- 559 [38] R. Ranjbarzadeh, S. B. Saadi, and A. Amirabadi, “LNPSS: SAR image despeckling based
560 on local and non-local features using patch shape selection and edges linking,” *Meas. J. Int.*
561 *Meas. Confed.*, vol. 164, Nov. 2020, doi: 10.1016/j.measurement.2020.107989.
- 562 [39] Y. Tang and X. Wu, “Scene text detection using superpixel-based stroke feature transform
563 and deep learning based region classification,” *IEEE Trans. Multimed.*, vol. 20, no. 9, pp.
564 2276–2288, Sep. 2018, doi: 10.1109/TMM.2018.2802644.
- 565 [40] G. Nalcaci, A. Özmen, and G. W. Weber, “Long-term load forecasting: models based on
566 MARS, ANN and LR methods,” *Cent. Eur. J. Oper. Res.*, vol. 27, no. 4, pp. 1033–1049,
567 Dec. 2019, doi: 10.1007/S10100-018-0531-1/FIGURES/9.
- 568 [41] S. Shamshirband, P. Saraei, N. Nabipour, and A. Baghban, “Hydrocarbons density
569 estimates for a wide range of conditions using RBF-ANN and ANFIS strategies,” 2019, doi:
570 10.1080/15567036.2019.1704313.
- 571 [42] M. Turab, T. Kumar, M. Bendechache, and T. Saber, “Investigating Multi-Feature Selection
572 and Ensembling for Audio Classification,” Jun. 2022, doi: 10.48550/arxiv.2206.07511.
- 573 [43] G. R. Kanagachidambaresan, A. Ruwali, D. Banerjee, and K. B. Prakash, “Recurrent Neural
574 Network,” in *EAI/Springer Innovations in Communication and Computing*, Springer
575 Science and Business Media Deutschland GmbH, 2021, pp. 53–61.
- 576 [44] S. M. Mousavi, A. Asgharzadeh-Bonab, and R. Ranjbarzadeh, “Time-Frequency Analysis
577 of EEG Signals and GLCM Features for Depth of Anesthesia Monitoring,” *Comput. Intell.*
578 *Neurosci.*, vol. 2021, pp. 1–14, Aug. 2021, doi: 10.1155/2021/8430565.
- 579 [45] J. Ma et al., “Arbitrary-oriented scene text detection via rotation proposals,” *IEEE Trans.*
580 *Multimed.*, vol. 20, no. 11, pp. 3111–3122, Nov. 2018, doi: 10.1109/TMM.2018.2818020.
- 581 [46] P. Shivakumara, R. Raghavendra, L. Qin, K. B. Raja, T. Lu, and U. Pal, “A new multi-
582 modal approach to bib number/text detection and recognition in Marathon images,” *Pattern*
583 *Recognit.*, vol. 61, pp. 479–491, Jan. 2017, doi: 10.1016/j.patcog.2016.08.021.
- 584 [47] M. Liao, Z. Zou, Z. Wan, C. Yao, and X. Bai, “Real-Time Scene Text Detection with

- 585 Differentiable Binarization and Adaptive Scale Fusion,” *IEEE Trans. Pattern Anal. Mach.*
586 *Intell.*, 2022, doi: 10.1109/TPAMI.2022.3155612.
- 587 [48] W. He, X. Y. Zhang, F. Yin, Z. Luo, J. M. Ogier, and C. L. Liu, “Realtime multi-scale scene
588 text detection with scale-based region proposal network,” *Pattern Recognit.*, vol. 98, p.
589 107026, Feb. 2020, doi: 10.1016/j.patcog.2019.107026.
- 590 [49] G. Tong, M. Dong, X. Sun, and Y. Song, “Natural scene text detection and recognition
591 based on saturation-incorporated multi-channel MSER,” *Knowledge-Based Syst.*, vol. 250,
592 p. 109040, Aug. 2022, doi: 10.1016/J.KNOSYS.2022.109040.
- 593 [50] S. Hong, B. Roh, K.-H. Kim, Y. Cheon, and M. Park, “PVANet: Lightweight Deep Neural
594 Networks for Real-time Object Detection,” Nov. 2016, Accessed: Dec. 26, 2020. [Online].
595 Available: <http://arxiv.org/abs/1611.08588>.
- 596 [51] W. Shang, K. Sohn, D. Almeida, and H. Lee, “Understanding and Improving Convolutional
597 Neural Networks via Concatenated Rectified Linear Units,” *33rd Int. Conf. Mach. Learn.*
598 *ICML 2016*, vol. 5, pp. 3276–3284, Mar. 2016, Accessed: Dec. 26, 2020. [Online].
599 Available: <http://arxiv.org/abs/1603.05201>.
- 600 [52] S. J. Ghouschi, R. Ranjbarzadeh, A. H. Dadkhah, Y. Pourasad, and M. Bendeche, “An
601 Extended Approach to Predict Retinopathy in Diabetic Patients Using the Genetic
602 Algorithm and Fuzzy C-Means,” *Biomed Res. Int.*, vol. 2021, pp. 1–13, Jun. 2021, doi:
603 10.1155/2021/5597222.
- 604 [53] T. He, W. Huang, Y. Qiao, and J. Yao, “Text-Attentional Convolutional Neural Network
605 for Scene Text Detection,” *IEEE Trans. Image Process.*, vol. 25, no. 6, pp. 2529–2541, Jun.
606 2016, doi: 10.1109/TIP.2016.2547588.
- 607 [54] S. Anari, N. Tataei Sarshar, N. Mahjoori, S. Dorosti, and A. Rezaie, “Review of Deep
608 Learning Approaches for Thyroid Cancer Diagnosis,” *Math. Probl. Eng.*, vol. 2022, pp. 1–
609 8, Aug. 2022, doi: 10.1155/2022/5052435.
- 610 [55] K.-H. Kim, S. Hong, B. Roh, Y. Cheon, and M. Park, “PVANET: Deep but Lightweight
611 Neural Networks for Real-time Object Detection,” *ArXiv*, vol. 2012, pp. 1–7, Aug. 2016,
612 Accessed: Dec. 26, 2020. [Online]. Available: <http://arxiv.org/abs/1608.08021>.

- 613 [56] F. Naiemi, V. Ghods, and H. Khalesi, "A novel pipeline framework for multi oriented scene
614 text image detection and recognition," *Expert Syst. Appl.*, vol. 170, p. 114549, May 2021,
615 doi: 10.1016/j.eswa.2020.114549.
- 616 [57] Z. Zhong, L. Sun, and Q. Huo, "Improved localization accuracy by LocNet for Faster R-
617 CNN based text detection in natural scene images," *Pattern Recognit.*, vol. 96, p. 106986,
618 Dec. 2019, doi: 10.1016/j.patcog.2019.106986.
- 619 [58] C. Szegedy et al., "Going Deeper with Convolutions," 2015.
- 620 [59] C. Szegedy, V. Vanhoucke, S. Ioffe, and J. Shlens, "Rethinking the Inception Architecture
621 for Computer Vision," 2016.
- 622 [60] R. Ranjbarzadeh, A. Bagherian Kasgari, S. Jafarzadeh Ghouschi, S. Anari, M. Naseri, and
623 M. Bendeche, "Brain tumor segmentation based on deep learning and an attention
624 mechanism using MRI multi-modalities brain images," *Sci. Rep.*, vol. 11, no. 1, p. 10930,
625 Dec. 2021, doi: 10.1038/s41598-021-90428-8.
- 626 [61] S. Baseri Saadi, N. Tataei Sarshar, S. Sadeghi, R. Ranjbarzadeh, M. Kooshki Forooshani,
627 and M. Bendeche, "Investigation of Effectiveness of Shuffled Frog-Leaping Optimizer
628 in Training a Convolution Neural Network," *J. Healthc. Eng.*, vol. 2022, pp. 1–11, Mar.
629 2022, doi: 10.1155/2022/4703682.
- 630 [62] D. Karatzas et al., "ICDAR 2013 robust reading competition," in *Proceedings of the
631 International Conference on Document Analysis and Recognition, ICDAR, 2013*, pp. 1484–
632 1493, doi: 10.1109/ICDAR.2013.221.
- 633 [63] D. Karatzas et al., "ICDAR 2015 competition on Robust Reading," in *Proceedings of the
634 International Conference on Document Analysis and Recognition, ICDAR, Nov. 2015*, vol.
635 2015-November, pp. 1156–1160, doi: 10.1109/ICDAR.2015.7333942.
- 636 [64] N. Nayef et al., "ICDAR2017 Robust Reading Challenge on Multi-Lingual Scene Text
637 Detection and Script Identification - RRC-MLT," in *Proceedings of the International
638 Conference on Document Analysis and Recognition, ICDAR, Jul. 2017*, vol. 1, pp. 1454–
639 1459, doi: 10.1109/ICDAR.2017.237.
- 640 [65] N. Nayef et al., "ICDAR2019 robust reading challenge on multi-lingual scene text detection

- 641 and recognition-RRC-MLT-2019,” in Proceedings of the International Conference on
642 Document Analysis and Recognition, ICDAR, Sep. 2019, pp. 1582–1587, doi:
643 10.1109/ICDAR.2019.00254.
- 644 [66] S. Saha et al., “Multi-lingual scene text detection and language identification,” *Pattern*
645 *Recognit. Lett.*, vol. 138, pp. 16–22, Oct. 2020, doi: 10.1016/j.patrec.2020.06.024.
- 646 [67] A. Fateh, M. Rezvani, A. Tajary, and M. Fateh, “Persian printed text line detection based
647 on font size,” *Multimed. Tools Appl.*, pp. 1–26, Jun. 2022, doi: 10.1007/S11042-022-
648 13243-X/FIGURES/17.
- 649 [68] F. Tasnim, S. U. Habiba, N. Nafisa, and A. Ahmed, “Depressive Bangla Text Detection
650 from Social Media Post Using Different Data Mining Techniques,” *Lect. Notes Electr. Eng.*,
651 vol. 834, pp. 237–247, 2022, doi: 10.1007/978-981-16-8484-5_21/COVER.
- 652 [69] M. Liao, B. Shi, X. Bai, X. Wang, and W. Liu, “TextBoxes: A Fast Text Detector with a
653 Single Deep Neural Network,” *31st AAAI Conf. Artif. Intell. AAAI 2017*, pp. 4161–4167,
654 Nov. 2016, Accessed: Dec. 24, 2020. [Online]. Available: <http://arxiv.org/abs/1611.06779>.
- 655 [70] Z. Zhong, L. Sun, and Q. Huo, “An anchor-free region proposal network for Faster R-CNN-
656 based text detection approaches,” in *International Journal on Document Analysis and*
657 *Recognition*, Sep. 2019, vol. 22, no. 3, pp. 315–327, doi: 10.1007/s10032-019-00335-y.
- 658 [71] L. Xie, Y. Liu, L. Jin, and Z. Xie, “DeRPN: Taking a further step toward more general
659 object detection,” in *33rd AAAI Conference on Artificial Intelligence, AAAI 2019, 31st*
660 *Innovative Applications of Artificial Intelligence Conference, IAAI 2019 and the 9th AAAI*
661 *Symposium on Educational Advances in Artificial Intelligence, EAAI 2019*, Jul. 2019, vol.
662 33, no. 01, pp. 9046–9053, doi: 10.1609/aaai.v33i01.33019046.
- 663 [72] S. Roy, P. Shivakumara, U. Pal, T. Lu, and G. H. Kumar, “Delaunay triangulation based
664 text detection from multi-view images of natural scene,” *Pattern Recognit. Lett.*, vol. 129,
665 pp. 92–100, Jan. 2020, doi: 10.1016/j.patrec.2019.11.021.
- 666 [73] B. Shi, X. Bai, and S. Belongie, “Detecting Oriented Text in Natural Images by Linking
667 Segments,” 2017.
- 668 [74] Z. Huang, Z. Zhong, L. Sun, and Q. Huo, “Mask R-CNN with pyramid attention network

669 for scene text detection,” in Proceedings - 2019 IEEE Winter Conference on Applications
670 of Computer Vision, WACV 2019, Mar. 2019, pp. 764–772, doi:
671 10.1109/WACV.2019.00086.

672 [75] S. X. Zhang, X. Zhu, J. B. Hou, C. Yang, and X. C. Yin, “Kernel Proposal Network for
673 Arbitrary Shape Text Detection,” IEEE Trans. Neural Networks Learn. Syst., 2022, doi:
674 10.1109/TNNLS.2022.3152596.

675 [76] P. Lyu, C. Yao, W. Wu, S. Yan, and X. Bai, “Multi-Oriented Scene Text Detection via
676 Corner Localization and Region Segmentation,” 2018.

677 [77] W. Wang et al., “Shape Robust Text Detection with Progressive Scale Expansion Network,”
678 2019.

679 [78] P. Yang et al., “Instance Segmentation Network with Self-Distillation for Scene Text
680 Detection,” IEEE Access, vol. 8, 2020, doi: 10.1109/ACCESS.2020.2978225.

681 [79] Z. Zhong, L. Sun, and Q. Huo, “A teacher-student learning based born-again training
682 approach to improving scene text detection accuracy,” in Proceedings of the International
683 Conference on Document Analysis and Recognition, ICDAR, Sep. 2019, pp. 281–286, doi:
684 10.1109/ICDAR.2019.00053.

685 [80] C. Zhang et al., “Look More Than Once: An Accurate Detector for Text of Arbitrary
686 Shapes,” 2019.

687 [81] A. Yildiz, H. Zan, and S. Said, “Classification and analysis of epileptic EEG recordings
688 using convolutional neural network and class activation mapping,” Biomed. Signal Process.
689 Control, vol. 68, p. 102720, Jul. 2021, doi: 10.1016/J.BSPC.2021.102720.

690 [82] R. R. Selvaraju, M. Cogswell, A. Das, R. Vedantam, D. Parikh, and D. Batra, “Grad-CAM:
691 Visual Explanations From Deep Networks via Gradient-Based Localization.” pp. 618–626,
692 2017, Accessed: Oct. 29, 2021. [Online]. Available: <http://gradcam.cloudcv.org>.

693

694

695